J. Appl. Comput. Mech., 6(3) (2020) 699-712
DOI: 10.22055/JACM.2019.31137.1833

ISSN: 2383-4536
jacm.scu.ac.ir

M&MoCS

Shahid Chamran University of Ahvaz

Journal of Applied and Computational Mechanics

Research Paper

The Density-Driven Nanofluid Convection in an Anisotropic Porous Medium Layer with Rotation and Variable Gravity Field: A Numerical Investigation

Dhananjay Yadav

Department of Mathematical & Physical Sciences, University of Nizwa, Nizwa, P.O. Box 33, PC 616, Sultanate of Oman

Received September 19 2019; Revised December 18 2019; Accepted for publication December 18 2019.
Corresponding author: D. Yadav (dhananjay@unizwa.edu.om; dhananjayadav@gmail.com)

Abstract. In this study, a numerical examination of the significance of rotation and changeable gravitational field on the start of nanofluid convective movement in an anisotropic porous medium layer is shown. A model that accounts for the impact of Brownian diffusion and thermophoresis is used for nanofluid, while Darcy's law is taken for the porous medium. The porous layer is subjected to uniform rotation and changeable downward gravitational field which fluctuates with the height from the layer by linearly or parabolic. The higher-order Galerkin technique is applied to obtain the numerical solutions. The outcomes demonstrate that the rotation parameter T_D, the thermal anisotropy parameter η and the gravity variation parameter λ slow the beginning of convective motion, whereas the mechanical anisotropy parameter ξ, the nanoparticle Rayleigh-Darcy number R_{np}, the modified diffusivity ratio NA_{nf} and the modified nanofluid Lewis number Le_{nf} quick the start of convective motion. For instance, by rising the gravity variation parameter λ from zero to 1.4, the critical nanofluid thermal Rayleigh-Darcy number $R_{nf,c}$ and the critical wave number a_c boost maximum around 133% and 7%, respectively for linear variation of the gravity field, while it were 47% and 2.8% for parabolic variation of the gravity field. It is also observed that the system is more unstable for the parabolic variation of the gravity field.

Keywords: Nanofluids, Convective instability, Rotation, Variable gravity, Anisotropic porous medium.

1. Introduction

During the last few years, the analysis of the nanofluid convection in a porous medium has become more and more attractive because of its numerous applications in the cooling of nuclear arrangements, defense and space, oil and gas recovery field applications, chemical engineering, and biomedical applications, etc [1-8]. Nield and Kuznetsov [9] were the first who examined the nanofluid convective movement in a porous matrix by taking the consequences of Brownian and thermophoresis properties of nanoparticles. They found that nanofluid is unstable than the normal fluid. The impact of rotation on the arrival of nanofluid convection in a porous matrix was examined by Chand and Rana [10]. The expansion of the double-diffusive case was prepared by Sharma and Gupta [11]. The impact of the internal heating on the nanofluid convective motion in a porous matrix was inspected by Yadav et al. [12-15], Nield and Kuznetsov [16] and Mahajan and Sharma [17] under different situations. They established that the inner heat resource rapids the start of nanofluid convection. The convective heat transport characteristics of CNT-water nanofluid in a cubic enclosure alienated with a rotating circular cylinder were studied by Selimefendigil and Öztop [18]. They showed that the average Nusselt number augmented approximately 18% at the maximum rotational speed as compared to the arrangement with

Published online: January 07 2020

motionless cylinder. Hadavand et al. [19] investigated the consequence of the attacking angle of the inclined cavity on mixed flow and heat transport of H_2O-Ag nanofluid numerically. They showed that the Nusselt number diminished more than 40% with an increase in the angle of attack to 45° and 90°. Very recently, Yadav [20] examined the convective heat transmit of nanofluids in porous enclosures and observed that the heat transfer enhanced 19.8% for W-Cu nanofluids as evaluated to the host fluid of water at 5% volumetric fraction of nanoparticles. Some other connected investigations in various situations were made by Akbarzadeh [21], Akbarzadeh and Mahian [22], Yadav et al. [23-31], Chand et al. [32-35], Sheikholeslami et al. [36], Selimefendigil and Öztop [37-39], Umavathi et al. [40] and Shivakumara et al. [41].

It is distinguished that the gravitational field of the earth differs with elevation from its plane in numerous of the big-scale convective phenomenon that arises in the oceanic, the layer of the earth, and crystal growth [42-46]. In experimental examinations, we usually disregard this gravity deviation and suppose the gravity field as a steady. But, on a big scale, it is desirable to consider gravity as a changeable quantity. Alex and Patil [47] inspected the consequence of the linear variation of gravity strength on the beginning of convection in an anisotropic porous matrix. Govender [48] investigated the result of rotation in a porous matrix subjected to a linear variation of the gravity field. The analysis was presented for stationary convection. Mahabaleshwar et al. [49] examined the outcomes of the variable internal heat source and variable gravity on the start of convection in a porous matrix using only one-term Galerkin method. Very recently, Yadav [50] investigated the collective result of changeable gravitational force and throughflow on the beginning of convection in a porous layer and observed that both the throughflow and gravity disparity factors late the beginning of the convective movement.

To consider the relevance of nanofluids with variable gravity related to heat transfer problems in space sciences, heat pipes and geothermal power extraction [51-53], Li et al. [54] calculated the outcomes of gravity and changeable heat characteristics on nanofluid convective heat transmit. They found that by raising the value of gravitational force, the flow velocity augmented along the vertical way. This showed that the gravitational force has a huge impact on the improvement of heat transmitted. Chand et al. [55] considered the inception of nanofluid convection in an anisotropic porous medium subjected to linear variation of gravity filed by only one term Galerkin process. Recently, Mahajan and Sharma [56] considered the thermal convection in a magnetic nanofluid with the uneven gravity field. They found that the variable gravity force delays the arrival of convection.

We are not aware of any examinations on the convection of nanofluids in anisotropic porous media with inconsistent gravity field and rotation. Such studies may be helpful to address the problems related to contaminant transport in saturated soils, petroleum drilling, space science, crystals growth, solidification and centrifugal forming of metals and rotating equipment as discussed above. In view of the importance of such a consideration, the main intent of the current work is to explore the collective outcome of rotation and the changeable gravity field on the start of nanofluid convection in an anisotropic porous medium layer. A numerical solution of the governing equations is found by applying a higher-terms Galerkin method for two types of gravitational field variation: (a) linear $(G(z)=-z)$, and (b) parabolic $(G(z)=-z^2)$. This article is structured as follows: starting with a brief introduction in section 1, we give a mathematical formulation of the considered problem in section 2. In section 3, the process of the numerical solution is presented. Section 4 is devoted to the main results and discussion on the onset of convective nanofluid flow in an anisotropic porous medium layer with a variable gravity field and rotation. Lastly, this article ends with a conclusion and future scope in section 5.

2. Physical Model and Mathematical Formulation

Consider the nanofluid flooded anisotropic porous layer enclosed by two infinite horizontal parallel plates $z=0$ and $z=h$. The layer is subject to the uniform rotation regarding the upright axis at a uniform angular velocity $\mathbf{\Omega}(0,0,\Omega)$ and inconsistent gravity field $\mathbf{g}(z)$ which varies with z and acts in the opposite z-direction. The nanoparticle flux is assumed to be dying out on the plates and the temperatures at the bottom and top plates are supposed to be θ_1 and $\theta_2\,(\theta_2<\theta_1)$, respectively. The physical diagram of the arrangement is shown in Fig. 1. It is considered that the suspension of nanoparticles into the host fluid is to be diluted and stable. We also believed that Darcy's law and the Boussinesq approximation are valid, that the solid matrix and the saturating nanofluid are in local thermal equilibrium. The appropriate governing equations are [20, 23, 57]:

$$\nabla.\mathbf{q}=0\,, \tag{1}$$

$$\nabla P=-\mu_{nf}\tilde{\mathbf{K}}^{-1}\mathbf{q}-\rho_{nf_0}\left[1-\beta_\theta(\theta-\theta_0)+\beta_C(C-C_0)\right]g(z)\hat{\mathbf{e}}_\mathbf{z}+\frac{2\rho_0}{\varepsilon}(\mathbf{q}\times\mathbf{\Omega}), \tag{2}$$

$$\left[(\rho c)_m\frac{\partial}{\partial\tau}+(\rho c)_{nf}(\mathbf{q}\cdot\nabla)\right]\theta=\nabla\cdot\left(\tilde{\mathbf{k}}_m\cdot\nabla\theta\right), \tag{3}$$

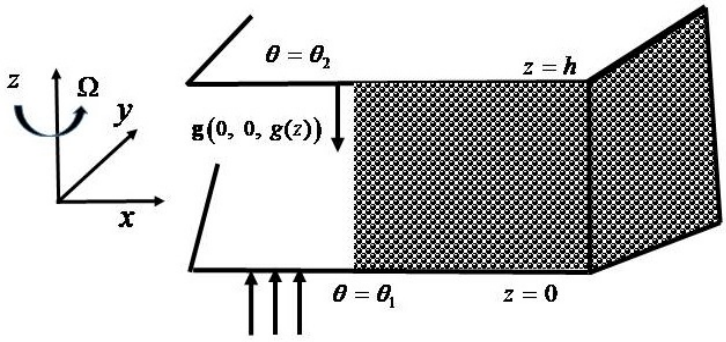

Fig. 1. Physical diagram of the considered system.

$$\left[\frac{\partial}{\partial\tau}+\frac{1}{\varepsilon}(\mathbf{q}.\nabla)\right]C=\nabla\cdot\left(\mathrm{D_B}\,\nabla C+\frac{\mathrm{D}_\theta}{\theta_0}\nabla\theta\right), \tag{4}$$

Here $g(z)=g_0\left[1+\lambda G(z)\right]$. All notation applied in the above equations is defined in nomenclature. In order to write the Eq. (3), we neglected the consequences of Brownian movement and thermophoresis because the ratio of the modified specific heat augmentation and the modified Lewis number are very small for nanofluids [58-60]. The thermal conductivity tensor $\tilde{\mathbf{k}}_m$ and the inverse of the permeability tensor $\tilde{\mathbf{K}}^{-1}$ of the porous medium are defined as:

$$\tilde{\mathbf{k}}_m=k_{mx}\left(\hat{\mathbf{e}}_\mathbf{x}\hat{\mathbf{e}}_\mathbf{x}+\hat{\mathbf{e}}_\mathbf{y}\hat{\mathbf{e}}_\mathbf{y}\right)+k_{mz}\hat{\mathbf{e}}_\mathbf{z}\hat{\mathbf{e}}_\mathbf{z}\,, \tag{5}$$

$$\tilde{\mathbf{K}}^{-1}=K_x^{-1}\left(\hat{\mathbf{e}}_\mathbf{x}\hat{\mathbf{e}}_\mathbf{x}+\hat{\mathbf{e}}_\mathbf{y}\hat{\mathbf{e}}_\mathbf{y}\right)+K_z^{-1}\hat{\mathbf{e}}_\mathbf{z}\hat{\mathbf{e}}_\mathbf{z}\,, \tag{6}$$

On applying the following replacement: $\theta=\hat{\theta}\Delta\theta+\theta_0$, $(x,y,z)=h(\bar{x},\bar{y},\bar{z})$, $\mathbf{q}=k_v\,\bar{\mathbf{q}}/h$, $\tau=\varepsilon h^2\,\bar{\tau}/k_v$, $C=\hat{C}C_0+C_0$, $P=\mu_{nf}k_v\,\bar{P}/K_z$, $k_v=k_{mz}/\left((\rho c)_{nf}\right)$, $\Delta\theta=(\theta_1-\theta_2)$, Eqs. (1)-(4) after eliminating the pressure term and taking the vertical component are (after ignoring the tie superscripts for simplicity):

$$\nabla_H^2 w+\frac{1}{\xi}\frac{\partial^2 w}{\partial z^2}-\left[R_{nf}\nabla_H^2\theta-R_{np}\nabla_H^2 C\right]\left[1+\lambda G(z)\right]+T_D\frac{\partial^2 w}{\partial z^2}=0, \tag{7}$$

$$\gamma\frac{\partial\theta}{\partial\tau}+(\mathbf{q}\cdot\nabla)\theta=\left(\eta\nabla_H^2+\frac{\partial^2}{\partial z^2}\right)\theta\,, \tag{8}$$

$$\frac{\partial C}{\partial\tau}+(\mathbf{q}\cdot\nabla)C=\frac{1}{Le_{nf}}\nabla^2 C+\frac{NA_{nf}}{Le_{nf}}\nabla^2\theta\,, \tag{9}$$

Here, $\nabla=\hat{\mathbf{e}}_\mathbf{x}\,\partial/\partial x+\hat{\mathbf{e}}_\mathbf{y}\,\partial/\partial y+\hat{\mathbf{e}}_\mathbf{z}\,\partial/\partial z$, $\nabla^2=\partial^2/\partial x^2+\partial^2/\partial y^2+\partial^2/\partial z^2$, $\nabla_H^2=\partial^2/\partial x^2+\partial^2/\partial y^2$, $\mathrm{Le_{nf}}=k_v/(\varepsilon D_B)$, $\xi=K_x/K_z$, $\eta=k_{mx}/k_{mz}$, $\mathrm{R_{nf}}=(\rho\beta_\theta)_{nf_0}\,hK_z g_0\Delta\theta/\left(\mu_{nf}k_v\right)$, $\mathrm{T_D}=(2\rho_0 K_z\Omega/\varepsilon\mu)^2$, $\mathrm{R_{np}}=\left(\rho\beta_C\right)_{nf_0}C_0K_z hg_0/\left(\mu_{nf}k_v\right)$, $\gamma=\left(\rho c\right)_m/\left(\varepsilon(\rho c)_{nf}\right)$ and $\mathrm{NA_{nf}}=D_\theta\Delta\theta/\left(\theta_c D_B C_0\right)$. The boundary circumstances in the non-dimension form are:

$$\begin{aligned} &w=0,\ \theta=1,\ \partial C/\partial\mathrm{z}+\mathrm{NA_{nf}}\,\partial\theta/\partial\mathrm{z}=0,\ \text{at } z=0,\\ &w=0,\ \theta=0,\ \ \partial C/\partial\mathrm{z}+\mathrm{NA_{nf}}\,\partial\theta/\partial\mathrm{z}=0,\ \text{at } z=1. \end{aligned} \tag{10}$$

It is supposed that the basic state to be dormant and of the form: $\mathbf{q}_b=(0,0,0)$, $\theta_b=\theta_b(z)$, $C_\mathrm{b}=C_\mathrm{b}(z)$. Then, the basic temperature and concentration fields are:

$$\theta_b=1-z\,, \tag{11}$$

$$C_b = \mathrm{NA}_{\mathrm{nf}}\left(z-0.5\right), \tag{12}$$

Now, the basic state is perturbed as:

$$\mathbf{q} = \mathbf{q}_b + \mathbf{q}',\ \theta = \theta_{\mathrm{b}} + \theta',\ C = C_{\mathrm{b}} + C', \tag{13}$$

where $\mathbf{q}'$, θ' and C' are the perturbed quantities and supposed to be small. Using the above into Eqs. (7)-(9) and linearizing, we can write the stability equations as:

$$\nabla_H^2 w' + \frac{1}{\xi}\frac{\partial^2 w'}{\partial z^2} + \mathrm{T_D}\frac{\partial^2 w'}{\partial z^2} - \left[\mathrm{R_{nf}}\nabla_H^2\theta' - \mathrm{R_{np}}\nabla_H^2 C'\right]\left[1+\lambda G(z)\right] = 0, \tag{14}$$

$$\gamma\frac{\partial\theta'}{\partial\tau} + \left(\mathbf{q}'\cdot\nabla\right)\theta_b + \left(\mathbf{q}_b\cdot\nabla\right)\theta' = \left(\eta\nabla_H^2 + \frac{\partial^2}{\partial z^2}\right)\theta', \tag{15}$$

$$\frac{\partial C'}{\partial\tau} + \left(\mathbf{q}'\cdot\nabla\right)C_b + \left(\mathbf{q}_b\cdot\nabla\right)C' = \frac{1}{\mathrm{Le_{nf}}}\nabla^2 C' + \frac{\mathrm{NA_{nf}}}{\mathrm{Le_{nf}}}\nabla^2\theta'. \tag{16}$$

We suppose the perturbed quantities satisfying the relevant boundary conditions as [45]:

$$\left(w',\ \theta',\ C'\right) = \left[\hat{w}(z),\ \hat{\theta}(z),\ \hat{C}(z)\right]\mathrm{e}^{i(\kappa x+\chi y)+\sigma\tau}, \tag{17}$$

where κ and χ are the flat wave numbers and $\sigma = \sigma_r + i\sigma_i$ is the augmentation rate of volatility. Applying Eq. (17) into Eqs. (14)-(16), we get:

$$\left[\frac{1}{\xi}D^2 - a^2 + \mathrm{T_D}D^2\right]\hat{w} + \left[a^2\mathrm{R_{nf}}\hat{\theta} - a^2\mathrm{R_{np}}\hat{C}\right]\left[1+\lambda G(z)\right] = 0, \tag{18}$$

$$-\frac{d\theta_b}{dz}\hat{w} + \left[D^2 - \eta a^2 - \gamma\sigma\right]\hat{\theta} = 0, \tag{19}$$

$$-\frac{dC_b}{dz}\hat{w} + \frac{\mathrm{NA_{nf}}}{\mathrm{Le_{nf}}}\left(D^2 - a^2\right)\hat{\theta} + \left[\frac{1}{\mathrm{Le_{nf}}}\left(D^2 - a^2\right) - \sigma\right]\hat{C} = 0, \tag{20}$$

where $d/dz \equiv D$ and $a = \sqrt{\kappa^2 + \chi^2}$. In the perturbation dimensionless form, the boundary positions converted into:

$$\hat{w} = D\hat{w} = 0, \hat{\theta} = 0,\ D\hat{C} + \mathrm{NA_{nf}}D\hat{\theta} = 0 \ \text{ at } \ z = 0,1, \tag{21}$$

3. Process of Solution

The system of linear equations (18)–(20) is cracked numerically by means of the Galerkin process. Therefore, the variables are considered:

$$\hat{w} = \sum_{k=1}^{N} A_k\hat{w}_k,\ \hat{\theta} = \sum_{k=1}^{N} B_k\hat{\theta}_k, \text{ and } \hat{C} = \sum_{k=1}^{N} E_k\hat{C}_k, \tag{22}$$

Here A_k, B_k and E_k are constant and, $\hat{w}_k$, $\hat{\theta}_k$ and $\hat{C}_k$ are assumed as:

$$\hat{w}_k = \hat{\theta}_k = \sin k\pi z, \quad \hat{C}_k = -\mathrm{NA_{nf}}\sin k\pi z. \tag{23}$$

Using Eq. (23) into Eqs. (18)-(20) and utilizing the orthogonal property, we find the following system of algebraic equations:

Table 1. The contrast of $R_{nf,c}$ and a_c with λ for regular fluid in the nonexistence of internal heating and flow in an isotropic porous medium for (a) $G(z) = -z$ and (b) $G(z) = -z^2$.

		Current study		Rionero and Straughan [64]	
$G(z)$	λ	$R_{nf,c}$	a_c^2	$R_{nf,c}$	a_c^2
Case: (a)	0	39.478	9.872	39.478	9.870
	1	77.080	10.208	77.020	10.209
	1.5	132.020	12.313	132.020	12.314
	1.8	189.908	17.198	189.908	17.198
	1.9	212.281	19.475	212.280	19.470
Case: (b)	0	39.478	9.872	39.478	9.870
	0.2	41.832	9.872	41.832	9.874
	0.4	44.455	9.885	44.455	9.887
	0.6	47.389	9.916	47.389	9.915
	0.8	50.682	9.960	50. 682	9.961
	1	54.390	10.036	54.390	10.034

Table 2. Evaluation of $R_{nf,c}$ and a_c for various estimates of T_D and λ at R_{np}=1, NA_{nf}=3, Le_{nf}=10, $\xi = 0.7$ and $\eta = 0.6$ for cases (a) $G(z) = -z$ and (b) $G(z) = -z^2$.

T_D	λ	For case: (a)		For case: (b)		λ	For case: (a)		For case: (b)	
		$R_{nf,c}$	a_c	$R_{nf,c}$	a_c		$R_{nf,c}$	a_c	$R_{nf,c}$	a_c
0		10.6548	3.6016	10.6548	3.6016		34.4864	3.7474	21.0921	3.6840
50		401.8922	9.5127	401.8922	9.5127		675.0247	9.6467	521.3187	9.5922
100		742.6340	11.2986	742.6340	11.2986		1233.9449	11.4651	957.4229	11.3979
150	0	1073.0340	12.4994	1073.0340	12.4994	0.8	1775.7040	12.6911	1380.1940	12.6140
200		1398.0630	13.4292	1398.0630	13.4292		2308.5196	13.6416	1796.0262	13.5564
250		1719.6551	14.1983	1719.6551	14.1983		2835.6024	14.4283	2207.4138	14.3361
300		2038.8041	14.8596	2038.8041	14.8596		3358.6057	15.1049	2615.6400	15.0067
0		19.7815	3.6643	15.2951	3.6378		61.0022	3.9138	28.4308	3.7496
50		506.8780	9.5387	455.1926	9.5315		971.6283	10.0613	603.9730	9.7292
100		931.7775	11.3269	838.6328	11.3202		1763.2230	12.0001	1105.2746	11.5757
150	0.4	1343.7868	12.5305	1210.4305	12.5236	1.2	2529.3116	13.3105	1590.9850	12.8210
200		1749.0926	13.4628	1576.1765	13.4557		3282.0683	14.3272	2068.5684	13.7865
250		2150.1059	14.2341	1938.0486	14.2268		4026.2665	15.1690	2540.9419	14.5857
300		2548.0669	14.8974	2297.1663	14.8898		4764.3688	15.8932	3009.6077	15.2730

$$\begin{aligned} &F_{jk}A_k + G_{jk}B_k + H_{jk}E_k = 0, \\ &J_{jk}A_k + K_{jk}B_k = \sigma L_{jk}B_k, \\ &M_{jk}A_k + N_{jk}B_k + O_{jk}E_k = \sigma P_{jk}E_k. \end{aligned} \tag{24}$$

Here, $F_{jk} = \left\langle D\hat{w}_j D\hat{w}_k/\xi - a^2\hat{w}_j\hat{w}_k + T_D D\hat{w}_j D\hat{w}_k \right\rangle$, $G_{jk} = \left\langle a^2 R_{nf}\hat{w}_j\hat{\theta}_k\left[1+\lambda G(z)\right]\right\rangle$, $H_{jk} = \left\langle -a^2 R_{np}\hat{w}_j\hat{C}_k\left[1+\lambda G(z)\right]\right\rangle$,

$J_{jk} = \left\langle -\hat{\theta}_j\hat{w}_k D\theta_b \right\rangle$, $K_{jk} = \left\langle D\hat{\theta}_j D\hat{\theta}_k - \eta a^2\hat{\theta}_j\hat{\theta}_k \right\rangle$, $L_{jk} = \left\langle \gamma\hat{\theta}_j\hat{\theta}_k \right\rangle$, $M_{jk} = \left\langle -\hat{C}_j\hat{w}_k DC_b \right\rangle$, $N_{jk} = \left\langle NA_{nf}\left(D\hat{C}_j D\hat{\theta}_k - a^2\hat{C}_j\hat{\theta}_k\right)/Le_{nf} \right\rangle$,

$O_{jk} = \left\langle \left(D\hat{C}_j D\hat{C}_k - a^2\hat{C}_j\hat{C}_k\right)/Le_{nf} \right\rangle$, $P_{jk} = \left\langle \hat{C}_j\hat{C}_k \right\rangle$, where $\langle YZ\rangle = \int_0^1 YZdz$.

The above Eq. (24) is a generalized eigenvalue problem and solved in Matlab. Applying the QZ process, EIG function, Newton's technique and golden search procedure, the condition for the onset of natural convection are achieved in tenures of the critical nanofluid Rayleigh-Darcy number $R_{nf,c}$, the critical wave number a_c and the critical value of the frequency of oscillation $\sigma_{i,c}$.

4. Results and Discussion

In this part, the significance of consistent rotation and changeable gravitational field on the start of convective movement in an anisotropic porous layer saturated by nanofluid is presented via diagrams and tables. The results are obtained for two verities of gravitational field disparity: (a) linear, $G(z) = -z$ and (b) nonlinear, $G(z) = -z^2$ using the 7-terms Galerkin method for diverse values of control parameters. Based on the earlier investigations and existing data [61-63], the control parameters such as R_{np}, Le_{nf} and NA_{nf} are fixed in the range of $1 \sim 10$, $1 \sim 100$ and $1 \sim 10$, respectively. These ranges of the control parameters satisfy most of the nanofluids. For a choice of parametric values taken, it is found that σ_i is for all time zero viewing that the instability of the considered problem is stationary.

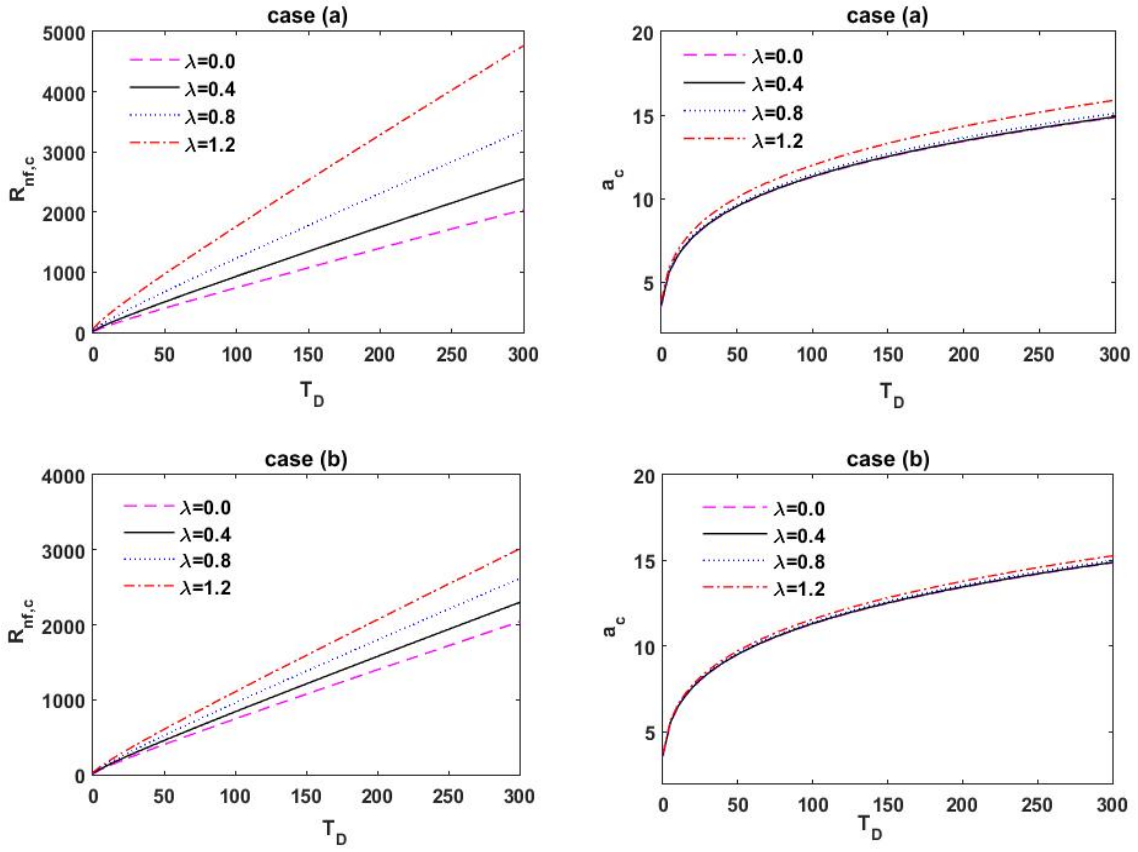

Fig. 2. Deviation of $R_{nf,c}$ and a_c with T_D for different values of λ at R_{np}=1, NA_{nf}=3, Le_{nf}=10, $\xi = 0.7$ and $\eta = 0.6$ for cases (a) $G(z) = -z$ and (b) $G(z) = -z^2$.

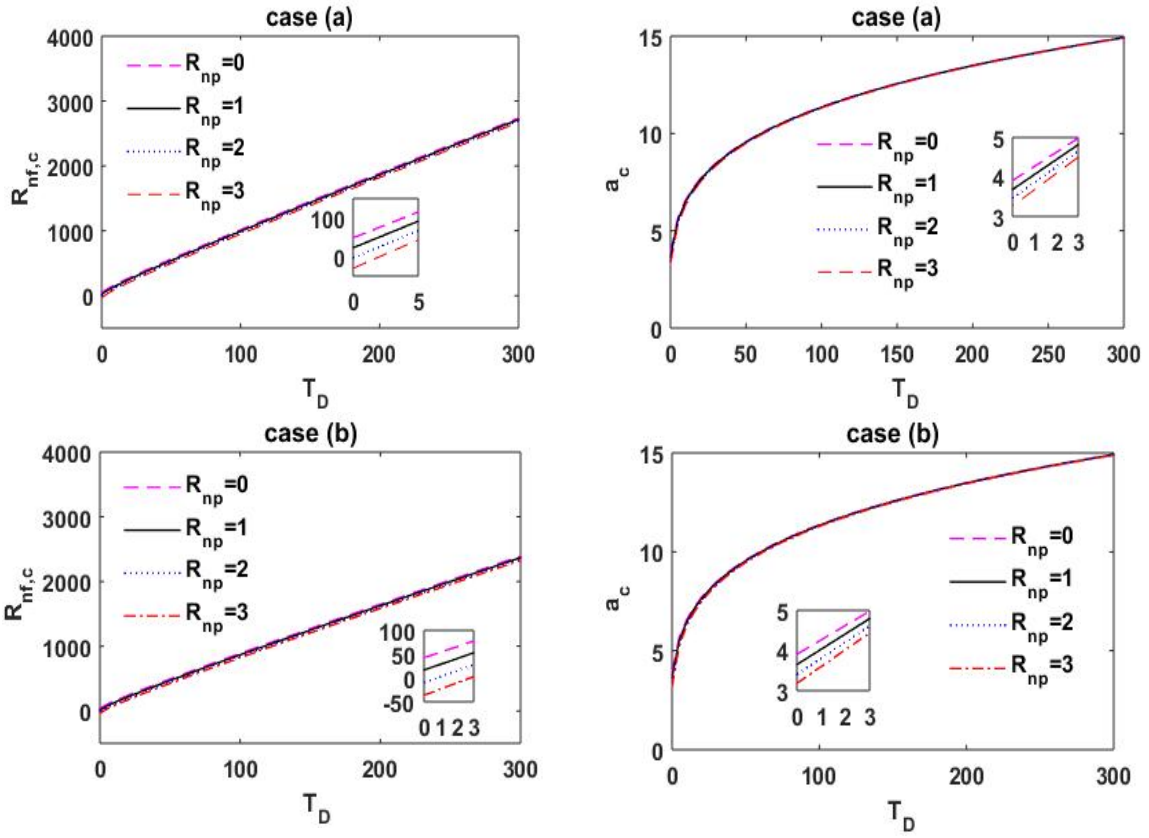

Fig. 3. Deviation of $R_{nf,c}$ and a_c with T_D for different values of R_{np} at $\lambda = 0.5$, NA_{nf}=3, Le_{nf}=10, $\xi = 0.7$ and $\eta = 0.6$ for cases (a) $G(z) = -z$ and (b) $G(z) = -z^2$.

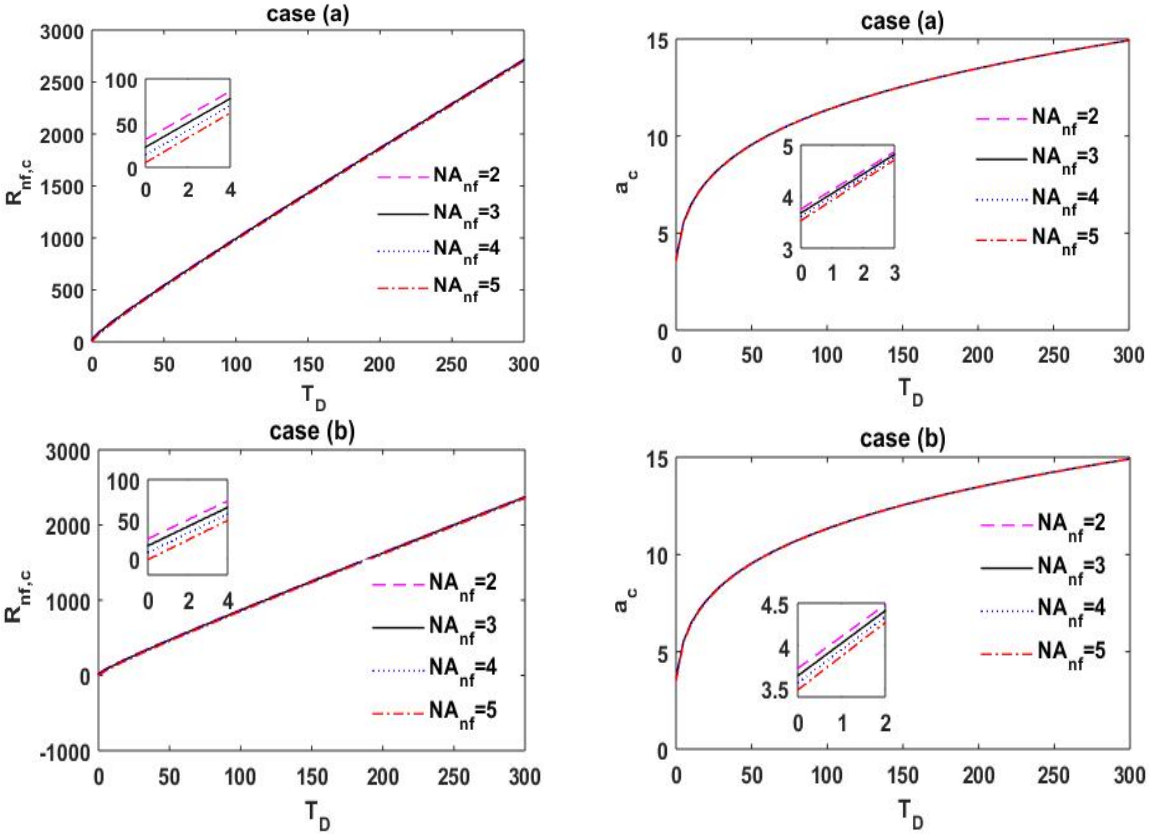

Fig. 4. Deviation of $R_{nf,c}$ and a_c with T_D for different values of NA_{nf} at R_{np}=1, Le_{nf}=10, $\xi = 0.7$, $\lambda = 0.5$ and $\eta = 0.6$ for cases (a) $G(z) = -z$ and (b) $G(z) = -z^2$.

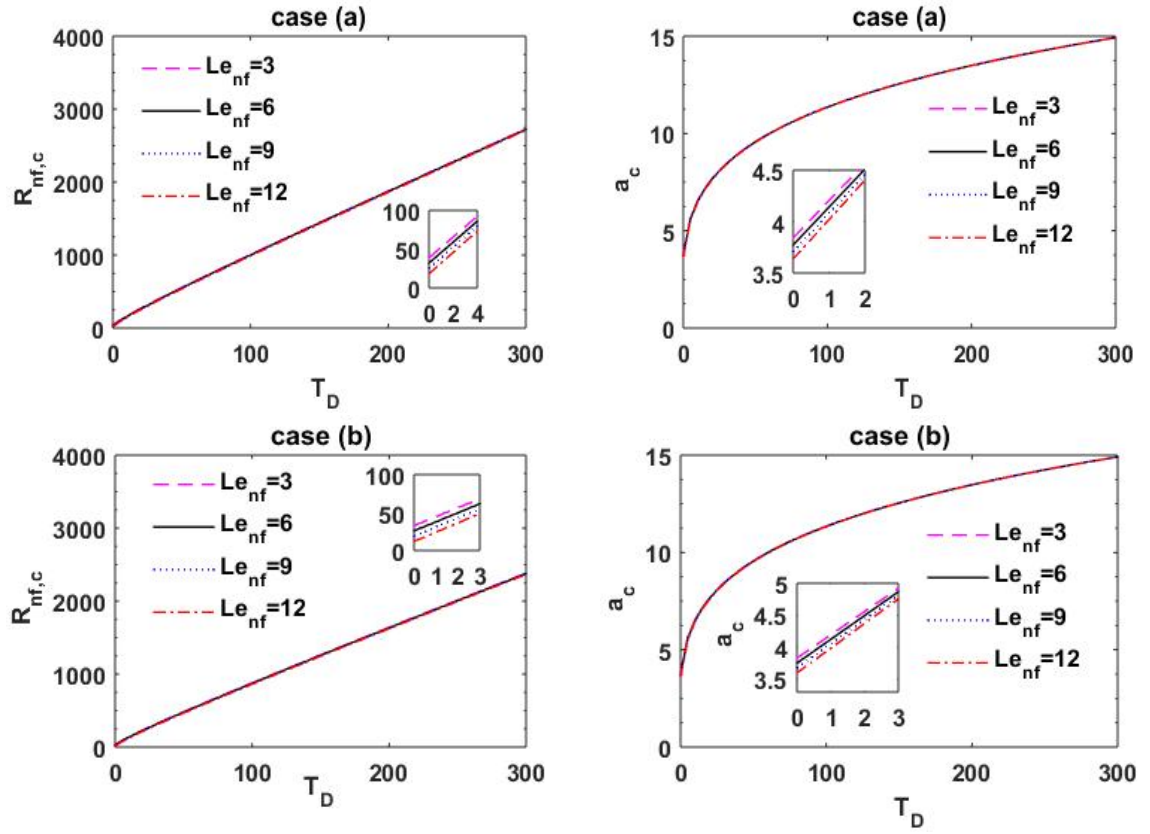

Fig. 5. Deviation of $R_{nf,c}$ and a_c with T_D for different values of Le_{nf} at R_{np}=1, NA_{nf}=3, $\xi = 0.7$, $\lambda = 0.5$ and $\eta = 0.6$ for cases (a) $G(z) = -z$ and (b) $G(z) = -z^2$.

Table 3. Evaluation of $R_{nf,c}$ and a_c for various estimates of T_D and R_{np} at $\lambda = 0.5$, NA_{nf}=3, Le_{nf}=10, $\xi = 0.7$ and $\eta = 0.6$ for cases (a) $G(z) = -z$ and (b) $G(z) = -z^2$.

T_D	R_{np}	For case: (a)		For case: (b)		R_{np}	For case: (a)		For case: (b)	
		$R_{nf,c}$	a_c	$R_{nf,c}$	a_c		$R_{nf,c}$	a_c	$R_{nf,c}$	a_c
0		48.6720	3.9101	42.5399	3.9083		-3.4664	3.4640	-9.7017	3.4024
50		563.4751	9.5886	492.5650	9.5816		519.1123	9.5187	448.2017	9.5015
100		1015.5836	11.3678	887.8249	11.3584		971.8565	11.3234	844.0985	11.3076
150	0	1454.1179	12.5689	1271.2304	12.5577	2	1410.6868	12.5352	1227.8003	12.5192
200		1885.5595	13.5005	1648.4423	13.4880		1842.3093	13.4729	1605.1930	13.4564
250		2312.4496	14.2719	2021.6797	14.2582		2269.3247	14.2482	1978.5557	14.2311
300		2736.0989	14.9355	2392.0873	14.9208		2693.0674	14.9147	2349.0568	14.8970
0		22.7799	3.6821	16.6226	3.6482		-30.0719	3.2627	-36.4350	3.1806
50		541.2976	9.5538	470.3878	9.5418		496.9191	9.4833	426.0065	9.4609
100		993.7216	11.3457	865.9635	11.3330		949.9882	11.3011	822.2298	11.2820
150	1	1432.4033	12.5520	1249.5164	12.5385	3	1388.9686	12.5182	1206.0821	12.4998
200		1863.9350	13.4867	1626.8183	13.4722		1820.6823	13.4590	1583.5663	13.4405
250		2290.8876	14.2600	2000.1182	14.2447		2247.7608	14.2364	1956.9922	14.2176
300		2714.5835	14.9251	2370.5725	14.9089		2671.5506	14.9042	2327.5404	14.8851

Table 4. Evaluation of $R_{nf,c}$ and a_c for various estimates of T_D and NA_{nf} at R_{np}=1, Le_{nf}=10, $\xi = 0.7$, $\lambda = 0.5$ and $\eta = 0.6$ for cases (a) $G(z) = -z$ and (b) $G(z) = -z^2$.

T_D	NA_{nf}	For case: (a)		For case: (b)		NA_{nf}	For case: (a)		For case: (b)	
		$R_{nf,c}$	a_c	$R_{nf,c}$	a_c		$R_{nf,c}$	a_c	$R_{nf,c}$	a_c
0		31.4493	3.7574	25.3062	3.7339		14.0710	3.6080	7.8937	3.5641
50		548.6910	9.5655	477.7811	9.5551		533.9034	9.5421	462.9934	9.5284
100		1001.0093	11.3531	873.2510	11.3415		986.4336	11.3383	858.6756	11.3246
150	2	1439.6417	12.5577	1256.7546	12.5449	4	1425.1647	12.5464	1242.2779	12.5320
200		1871.1433	13.4913	1634.0264	13.4775		1856.7265	13.4821	1619.6100	13.4669
250		2298.0750	14.2640	2007.3055	14.2492		2283.7000	14.2561	1992.9309	14.2402
300		2721.7553	14.9285	2377.7441	14.9129		2707.4115	14.9216	2363.4007	14.9049
0		22.7799	3.6821	16.6226	3.6482		5.3223	3.5352	-0.8811	3.4821
50		541.2976	9.5538	470.3878	9.5418		526.5083	9.5304	455.5980	9.5150
100		993.7216	11.3457	865.9635	11.3330		979.1452	11.3309	851.3872	11.3161
150	3	1432.4033	12.5520	1249.5164	12.5385	5	1417.9259	12.5408	1235.0392	12.5256
200		1863.9350	13.4867	1626.8183	13.4722		1849.5180	13.4775	1612.4016	13.4616
250		2290.8876	14.2600	2000.1182	14.2447		2276.5124	14.2522	1985.7433	14.2356
300		2714.5835	14.9251	2370.5725	14.9089		2700.2395	14.9181	2356.2287	14.9010

4.1 Numerical model and code validation

For the validation of present numerical model and code, first test computations are made for regular fluid in the absence of rotation and flow in an isotropic porous layer, i.e. $R_{np} = T_D = 0$, $\xi = \eta = 1$, and outcomes are contrasted with the previous outcomes that were presented by Rionero and Straughan [64] in Table 1. The comparison shows that the current numerical results are in superior conformity with the previously published outcomes. So, we are quite confident about the numerical outcomes of the current numerical code.

4.2 Significance of rotation and variable gravity field on the start of convection

Figure 2 shows the consequence of rotation parameter T_D and gravity variation parameter λ on $R_{nf,c}$ and a_c for cases (a) $G(z) = -z$ and (b) $G(z) = -z^2$. The outcomes are also given in Table 2. From these, it is found that $R_{nf,c}$ boosts with both T_D and λ. Hence, both parameters T_D and λ delay the start of convective activity. The critical nanofluid thermal Rayleigh-Darcy number $R_{nf,c}$ improves upon improving λ for the reason that; an increase in the estimate of λ supplies a lower in the gravitational force. Since the disturbance in the arrangement returns as the gravity force decreases and this shows to delay the start of the convective movement. The rotation parameter T_D has a stabilizing effect because rotation restrains the vertical movement and thus convection, by limiting the movement to the horizontal plane. The like result for rotation was also presented by Malashetty and Swamy [65].

4.3 Effect of nanoparticle parameters on the start of convection

The influences of the nanoparticle parameters such as R_{np}, NA_{nf} and Le_{nf} on the stability of the scheme are offered in Figs. 3, 4, and 5, respectively. The results are also presented in Tables 3, 4 and 5. From these, it is found that $R_{nf,c}$

diminishes on increasing R_{np}, NA_{nf} and Le_{nf}. Therefore, these factors have a destabilizing effect on the scheme. This happened because an augment in the values of R_{np}, NA_{nf} and Le_{nf} directs enhancing in the Brownian diffusion and thermophoresis of nanoparticles which carries the power of disorder in the arrangement. From these plots, it is also noted that the dimension of the convection cells augments on increasing R_{np}, NA_{nf} and Le_{nf}.

Table 5. Evaluation of $R_{nf,c}$ and a_c for various estimates of T_D and Le_{nf} at R_{np}=1, NA_{nf}=3, $\xi = 0.7$, $\lambda = 0.5$ and $\eta = 0.6$ for cases (a) $G(z) = -z$ and (b) $G(z) = -z^2$.

T_D	Le_{nf}	For case: (a)		For case: (b)		Le_{nf}	For case: (a)		For case: (b)	
		$R_{nf,c}$	a_c	$R_{nf,c}$	a_c		$R_{nf,c}$	a_c	$R_{nf,c}$	a_c
0		38.8407	3.8411	32.7064	3.8294		25.0848	3.7046	18.9324	3.6737
50		554.7227	9.5782	483.8127	9.5697		543.2157	9.5573	472.3059	9.5458
100		1006.9254	11.3612	879.1669	11.3508		995.6080	11.3479	867.8498	11.3356
150	3	1445.5037	12.5638	1262.6164	12.5519	9	1434.2748	12.5537	1251.3878	12.5404
200		1876.9723	13.4964	1639.8552	13.4832		1865.7975	13.4881	1628.6808	13.4738
250		2303.8811	14.2683	2013.1114	14.2541		2292.7438	14.2612	2001.9744	14.2460
300		2727.5443	14.9323	2383.5330	14.9172		2716.4350	14.9261	2372.4240	14.9101
0		31.9785	3.7726	25.8375	3.7512		18.1593	3.6375	11.9907	3.5975
50		548.9695	9.5678	478.0597	9.5577		537.4612	9.5468	466.5513	9.5337
100		1001.2668	11.3545	873.5085	11.3432		989.9489	11.3412	862.1908	11.3280
150	6	1439.8893	12.5588	1257.0022	12.5462	12	1428.6602	12.5487	1245.7733	12.5346
200		1871.3849	13.4922	1634.2680	13.4785		1860.2100	13.4839	1623.0934	13.4690
250		2298.3125	14.2648	2007.5429	14.2501		2287.1751	14.2577	1996.4058	14.2420
300		2721.9897	14.9292	2377.9785	14.9136		2710.8804	14.9230	2366.8694	14.9065

Table 6. Evaluation of $R_{nf,c}$ and a_c for various estimates of T_D and ξ at R_{np}=1, NA_{nf}=3, $Le_{nf} = 10$, $\lambda = 0.5$ and $\eta = 0.6$ for cases (a) $G(z) = -z$ and (b) $G(z) = -z^2$.

T_D	ξ	For case: (a)		For case: (b)		ξ	For case: (a)		For case: (b)	
		$R_{nf,c}$	a_c	$R_{nf,c}$	a_c		$R_{nf,c}$	a_c	$R_{nf,c}$	a_c
0		39.8937	4.3113	31.6943	4.2823		19.5957	3.5442	13.8110	3.5092
50		551.2450	9.6040	479.0855	9.5919		539.6381	9.5454	468.9368	9.5333
100		1003.2285	11.3758	874.2757	11.3632		992.1366	11.3406	864.5776	11.3280
150	0.4	1441.7125	12.5744	1257.6557	12.5608	0.8	1430.8514	12.5483	1248.1595	12.5347
200		1873.1259	13.5047	1634.8542	13.4902		1862.4030	13.4837	1625.4788	13.4692
250		2299.9974	14.2753	2008.0833	14.2599		2289.3691	14.2575	1998.7906	14.2421
300		2723.6334	14.9384	2378.4852	14.9222		2713.0750	14.9228	2369.2536	14.9067
0		26.8382	3.8471	20.2021	3.8145		14.8725	3.3238	9.6343	3.2874
50		543.5095	9.5650	472.3218	9.5530		537.3141	9.5335	466.9047	9.5215
100		995.8348	11.3524	867.8111	11.3398		989.9173	11.3335	862.6372	11.3209
150	0.6	1434.4723	12.5570	1251.3253	12.5434	1.0	1428.6787	12.5431	1246.2598	12.5295
200		1865.9776	13.4907	1628.6042	13.4762		1860.2581	13.4795	1623.6035	13.4650
250		2292.9121	14.2634	2001.8884	14.2481		2287.2432	14.2539	1996.9318	14.2386
300		2716.5947	14.9280	2372.3309	14.9118		2710.9632	14.9197	2367.4071	14.9036

Table 7. Evaluation of $R_{nf,c}$ and a_c for various estimates of T_D and η atR_{np}=1, NA_{nf}=3, $Le_{nf} = 10$, $\lambda = 0.5$ and $\xi = 0.7$ for cases (a) $G(z) = -z$ and (b) $G(z) = -z^2$.

T_D	η	For case: (a)		For case: (b)		η	For case: (a)		For case: (b)	
		$R_{nf,c}$	a_c	$R_{nf,c}$	a_c		$R_{nf,c}$	a_c	$R_{nf,c}$	a_c
0		18.7904	3.8858	13.6264	3.8222		26.5736	3.5442	19.4898	3.5290
50		385.4329	10.5490	334.8446	10.5331		693.1651	8.9091	602.4667	8.8999
100		696.1002	12.5396	606.4914	12.5244		1285.5858	10.5708	1120.4281	10.5601
150	0.4	995.4726	13.8777	868.2458	13.8620	0.8	1862.2354	11.6910	1624.6051	11.6791
200		1288.9830	14.9137	1124.8717	14.8973		2430.6614	12.5595	2121.5973	12.5464
250		1578.7433	15.7706	1378.2183	15.7535		2993.8154	13.2782	2613.9840	13.2642
300		1865.8381	16.5073	1629.2349	16.4895		3553.2177	13.8965	3103.0937	13.8816
0		22.7799	3.6821	16.6226	3.6482		30.2418	3.4414	22.2741	3.4397
50		541.2976	9.5538	470.3878	9.5418		842.4995	8.4417	732.3532	8.4349
100		993.7216	11.3457	865.9635	11.3330		1573.7882	10.0081	1371.7103	9.9990
150	0.6	1432.4033	12.5520	1249.5164	12.5385	1.0	2287.5463	11.0654	1995.7589	11.0548
200		1863.9350	13.4867	1626.8183	13.4722		2992.1449	11.8855	2611.8095	11.8736
250		2290.8876	14.2600	2000.1182	14.2447		3690.8659	12.5645	3222.7282	12.5516
300		2714.5835	14.9251	2370.5725	14.9089		4385.4020	13.1486	3829.9928	13.1348

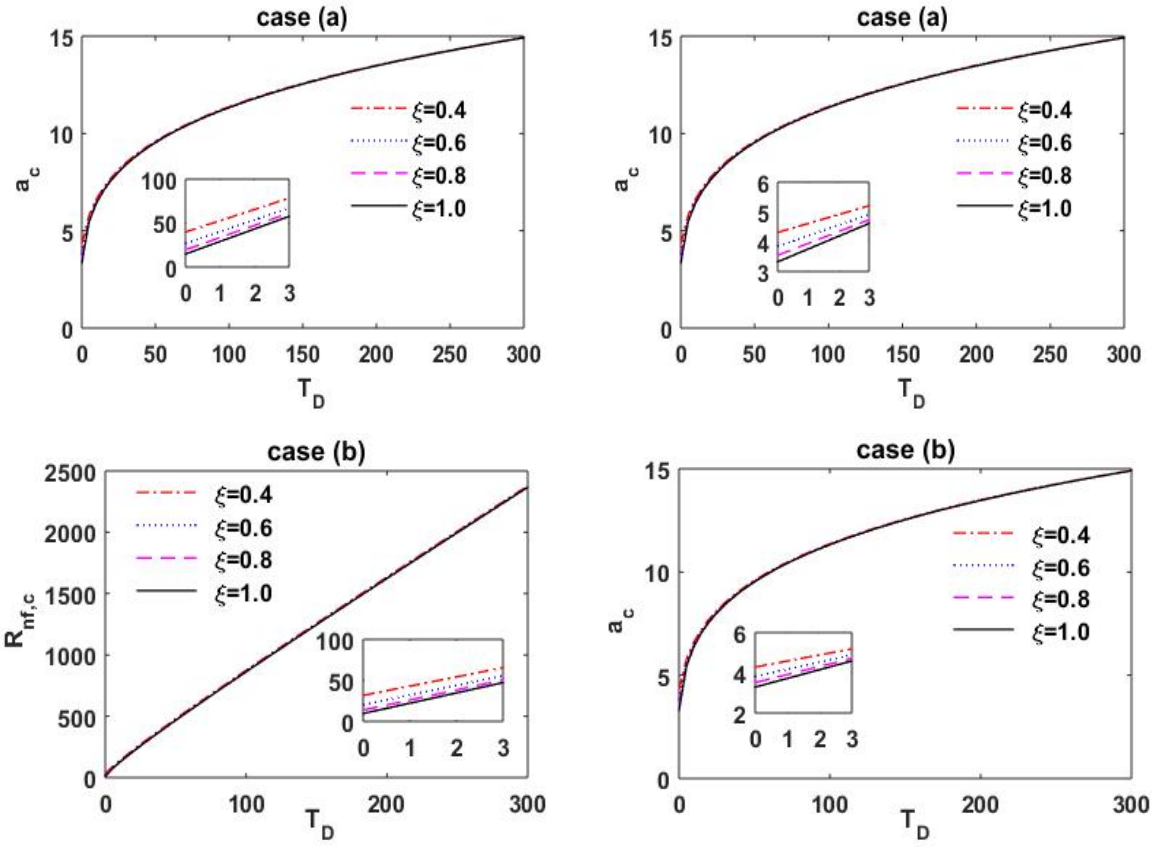

Fig. 6. Deviation of $R_{nf,c}$ and a_c with T_D for different values of ξ at R_{np}=1, NA_{nf}=3, $Le_{nf} = 10$, $\lambda = 0.5$ and $\eta = 0.6$ for cases (a) $G(z) = -z$ and (b) $G(z) = -z^2$.

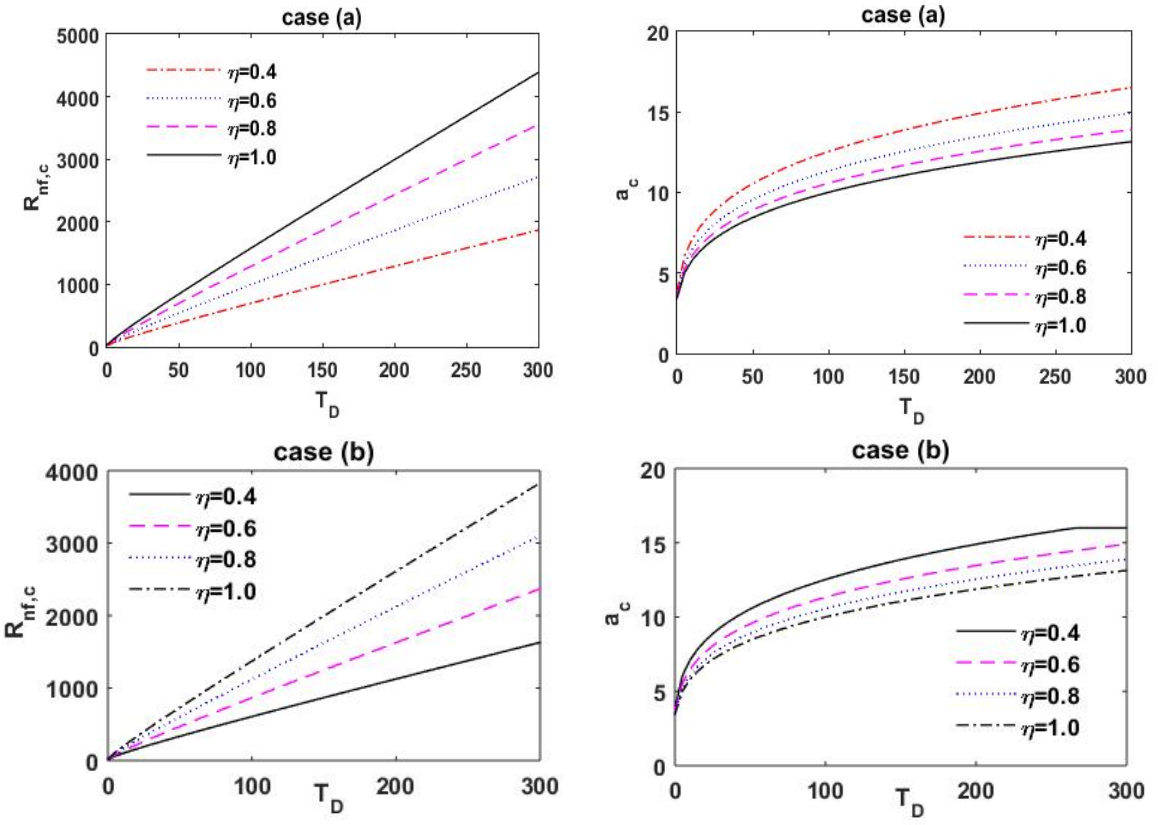

Fig. 7. Deviation of $R_{nf,c}$ and a_c with T_D for different values of η at R_{np}=1, NA_{nf}=3, $Le_{nf} = 10$, $\lambda = 0.5$ and $\xi = 0.7$ for cases (a) $G(z) = -z$ and (b) $G(z) = -z^2$.

4.4 Influence of mechanical anisotropy parameter on the launch of convection

Figure 6 and Table 6 show the result of ξ on the stability of the arrangement. It is noted that $R_{nf,c}$ reduced on rising ξ. For this reason, the impact of increasing ξ fasts the start of convective motion. This is because increasing ξ directs to larger horizontal permeability which fasts the movement of the fluid in the horizontal ways and hence lower values of $R_{nf,c}$ are preferred for the beginning of convection with increasing ξ. Additional, the dimension of the convection cells augments on rising ξ. This is because the small resistance to horizontal flow also guides to an extension of the horizontal wavelength.

4.5 Outcome of thermal anisotropy parameter on the start of convection

The influence of the thermal anisotropy parameter η on the stability of the arrangement is presented in Fig. 7 and Table 7. From these, it is found that $R_{nf,c}$ enhances on increase in the value of η, while a_c decreases on increasing η. This shows that η has a stabilizing result on the stability of the arrangement. This is because the horizontal thermal diffusivity augments with η.

5. Conclusion and Future Scope

In this paper, the significance of the consistent rotation and downward inconsistent gravity force on the arrival of nanofluid convection in an anisotropic porous matrix numerically were presented. The investigation was demonstrated for two cases of gravity force deviation: (a) linear $(G(z)=-z)$ and (b) nonlinear $(G(z)=-z^2)$. These allow us to draw the following conclusions:

- Effect of increasing T_D, η and λ delay the onset of convective motion, while ξ, R_{np}, NA_{nf} and Le_{nf} is found to quick the onset of convection.

- For example, by rising λ from zero to 1.4, the $R_{nf,c}$ and the a_c boost maximum around 133% and 7%, respectively for linear variation of a gravity field, while these were 47% and 2.8% for parabolic variation of gravity field.

- The dimension of the convective cells decreases on raising T_D and λ, while ξ, η, R_{np}, NA_{nf} and Le_{nf} increase the dimension of the convection cells.

- It is also observed that the arrangement is more unstable for case (b).

The present work can be extended for non-Newtonian nanofluids with or without rotation and magnetic field with different boundary conditions. An extension can also be made for variable thermophysical properties of nanofluids with a volumetric fraction of nanoparticles.

Acknowledgment

The author acknowledges the administration of the University of Nizwa for continuous support and encouragement.

Conflict of Interest

The author declared no potential conflicts of interest with respect to the research, authorship and publication of this article.

Funding

The author received no financial support for the research, authorship and publication of this article.

Nomenclature

a	dimensionless wave number	β_θ	thermal expansion coefficient $(1/K)$
C	concentration of nanoparticles	μ	viscosity $(Kg/(m.s))$
D_B	Brownian diffusion coefficient (m^2/s)	ρ	density (Kg/m^3)
D_θ	thermophoresis diffusion coefficient (m^2/s)	ε	porosity of the porous medium
$\hat{\mathbf{e}}$	unit vector	(ρc)	volumetric heat capacity $(J/(K.m^3))$
$g(z)$	variable gravity	σ	growth rate of instability

$G(z)$	the functional values for the variable gravity	λ	gravity variation parameter
g_0	reference gravity (m/s^2)	ξ	mechanical anisotropy parameter
h	dimensional nanofluid layer height (m)	η	thermal anisotropy parameter
$\tilde{K}$	permeability tensor of the porous medium (m^2)	τ	time (s)
$\tilde{\mathbf{k}}_m$	effective thermal conductivity tensor of porous medium $W/(m.K)$	θ	temperature (K)
$\mathrm{Le}_{\mathrm{nf}}$	modified nanofluid Lewis number	**Superscripts**	
$\mathrm{NA}_{\mathrm{nf}}$	modified diffusivity ratio	'	perturbed quantities
P	pressure (Pa)	**Subscripts**	
$\mathbf{q}$	velocity vector (m/s)	0	reference value
R_{nf}	nanofluid thermal Rayleigh-Darcy number	B	basic state
R_{np}	nanoparticle Rayleigh-Darcy number	c	critical
T_{D}	rotation parameter	m	effective porous medium
(x, y, z)	space co-ordinates (m)	nf	nanofluid
Greek symbols		np	nanoparticle
β_C	nanoparticle concentration expansion coefficient		

References

[1] B.A. Suleimanov, F. Ismailov, E. Veliyev, Nanofluid for enhanced oil recovery, *Journal of Petroleum Science and Engineering*, 78(2), 2011, 431-437.

[2] A. Kasaeian, R. Daneshazarian, O. Mahian, L. Kolsi, A.J. Chamkha, S. Wongwises, I. Pop, Nanofluid flow and heat transfer in porous media: a review of the latest developments, *International Journal of Heat and Mass Transfer*, 107, 2017, 778-791.

[3] R.A. Mahdi, H. Mohammed, K. Munisamy, N. Saeid, Review of convection heat transfer and fluid flow in porous media with nanofluid, *Renewable and Sustainable Energy Reviews*, 41, 2015, 715-734.

[4] A.I. Alsabery, A.J. Chamkha, H. Saleh, I. Hashim, Natural Convection Flow of a Nanofluid in an Inclined Square Enclosure Partially Filled With a Porous Medium, *Scientific Reports,* 7, 2017, 2357.

[5] W.C. Tan, L.H. Saw, H.S. Thiam, J. Xuan, Z. Cai, M.C. Yew, Overview of porous media/metal foam application in fuel cells and solar power systems, *Renewable and Sustainable Energy Reviews*, 96, 2018, 181-197.

[6] A. Asadi, A guideline towards easing the decision-making process in selecting an effective nanofluid as a heat transfer fluid, *Energy Conversion, and Management*, 175, 2018, 1-10.

[7] A. Asadi, F. Pourfattah, I.M. Szilágyi, M. Afrand, G. Zyla, H.S. Ahn, S. Wongwises, H.M. Nguyen, A. Arabkoohsar, O. Mahian, Effect of Sonication Characteristics on stability, thermophysical properties, and Heat Transfer of nanofluids: A Comprehensive Review, *Ultrasonics Sonochemistry*, 58, 2019, 104701.

[8] A. Asadi, I.M. Alarifi, V. Ali, H.M. Nguyen, An experimental investigation on the effects of ultrasonication time on stability and thermal conductivity of MWCNT-water nanofluid: Finding the optimum ultrasonication time, *Ultrasonics Sonochemistry*, 58, 2019, 104639.

[9] D.A. Nield, A.V. Kuznetsov, Thermal instability in a porous medium layer saturated by a nanofluid, *International Journal of Heat and Mass Transfer*, 52, 2009, 5796-5801.

[10] R. Chand, G.C. Rana, On the onset of thermal convection in rotating nanofluid layer saturating a Darcy–Brinkman porous medium, *International Journal of Heat and Mass Transfer*, 55, 2012, 5417-5424.

[11] J. Sharma, U. Gupta, Double-Diffusive Nanofluid Convection in Porous Medium with Rotation: Darcy-Brinkman Model, *Procedia Engineering*, 127, 2015,783-790.

[12] D. Yadav, R. Bhargava, G.S. Agrawal, Boundary and internal heat source effects on the onset of Darcy–Brinkman convection in a porous layer saturated by nanofluid, *International Journal of Thermal Sciences*, 60, 2012, 244-254.

[13] D. Yadav, J. Lee, H.H. Cho, Brinkman convection induced by purely internal heating in a rotating porous medium layer saturated by a nanofluid, *Powder Technology*, 286, 2015, 592-601.

[14] D. Yadav, Electrohydrodynamic Instability in a Heat Generating Porous Layer Saturated by a Dielectric Nanofluid, J. Appl. Fluid Mech., 10, 2017, 763-776.

[15] D. Yadav, The onset of longitudinal convective rolls in a porous medium saturated by a nanofluid with non-uniform internal heating and chemical reaction, *Journal of Thermal Analysis and Calorimetry*, 135, 2019, 1107-1117.

[16] D.A. Nield, A.V. Kuznetsov, Onset of convection with internal heating in a porous medium saturated by a nanofluid, *Transport in Porous Media*, 99, 2013, 73-83.

[17] A. Mahajan, M.K. Sharma, The onset of penetrative convection stimulated by internal heating in a magnetic nanofluid saturating a rotating porous medium, *Canadian Journal of Physics*, 96, 2017, 898-911.
[18] F. Selimefendigil, H.F. Öztop, Conjugate mixed convection of nanofluid in a cubic enclosure separated with a conductive plate and having an inner rotating cylinder, *International Journal of Heat and Mass Transfer*, 139, 2019, 1000-1017.
[19] M. Hadavand, S. Yousefzadeh, O.A. Akbari, F. Pourfattah, H.M. Nguyen, A. Asadi, A numerical investigation on the effects of mixed convection of Ag-water nanofluid inside a sim-circular lid-driven cavity on the temperature of an electronic silicon chip, *Applied Thermal Engineering*, 162, 2019, 114298.
[20] D. Yadav, Impact of chemical reaction on the convective heat transport in nanofluid occupying in porous enclosures: A realistic approach, *International Journal of Mechanical Sciences*, 157-158, 2019, 357-373.
[21] P. Akbarzadeh, The onset of MHD nanofluid convection between a porous layer in the presence of purely internal heat source and chemical reaction, *Journal of Thermal Analysis and Calorimetry*, 131, 2018, 2657-2672.
[22] P. Akbarzadeh, O. Mahian, The onset of nanofluid natural convection inside a porous layer with rough boundaries, *Journal of Molecular Liquids*, 272, 2018, 344-352.
[23] D. Yadav, G.S. Agrawal, R. Bhargava, Thermal instability of rotating nanofluid layer, *International Journal of Engineering Science*, 49, 2011, 1171-1184.
[24] D. Yadav, R. Bhargava, G.S. Agrawal, Numerical solution of a thermal instability problem in a rotating nanofluid layer, *International Journal of Heat and Mass Transfer*, 63, 2013, 313-322.
[25] D. Yadav, G.S. Agrawal, R. Bhargava, Onset of double-diffusive nanofluid convection in a layer of saturated porous medium with thermal conductivity and viscosity variation, *Journal of Porous Media*, 16, 2013, 105-121.
[26] D. Yadav, R. Bhargava, G.S. Agrawal, Thermal instability in a nanofluid layer with a vertical magnetic field, *Journal of Engineering Mathematics*, 80, 2013, 147-164.
[27] D. Yadav, R. Bhargava, G.S. Agrawal, G.S. Hwang, J. Lee, M.C. Kim, Magneto-convection in a rotating layer of nanofluid, *Asia-Pacific Journal of Chemical Engineering*, 9, 2014, 663-677.
[28] D. Yadav, Numerical solution of the onset of natural convection in a rotating nanofluid layer induced by purely internal heating, *International Journal of Applied and Computational Mathematics*, 3, 2017, 3663-3681.
[29] D. Yadav, R.A. Mohamed, J. Lee, H.H. Cho, Thermal convection in a Kuvshiniski viscoelastic nanofluid saturated porous layer, *Ain Shams Engineering Journal*, 8, 2017, 613-621.
[30] D. Yadav, A. Wakif, Z. Boulahia, R. Sehaqui, Numerical Examination of the Thermo-Electro-Hydrodynamic Convection in a Horizontal Dielectric Nanofluid Layer Using the Power Series Method, *Journal of Nanofluids*, 8, 2019, 1-15.
[31] D. Yadav, The effect of pulsating throughflow on the onset of magneto convection in a layer of nanofluid confined within a Hele-Shaw cell, *Proceedings of the Institution of Mechanical Engineers, Part E: Journal of Process Mechanical Engineering*, 233, 2019, 1074–1085.
[32] R. Chand, D. Yadav, G.C. Rana, Electrothermo convection in a horizontal layer of rotating nanofluid, *International Journal of Nanoparticles*, 8, 2015, 241-261.
[33] R. Chand, G.C. Rana, D. Yadav, Electrothermo convection in a porous medium saturated by nanofluid, *J. Appl. Fluid Mech.,* 9, 2016, 1081-1088.
[34] R. Chand, G.C. Rana, D. Yadav, Thermal Instability in a Layer of Couple Stress Nanofluid Saturated Porous Medium, *Journal of Theoretical and Applied Mechanics*, 47, 2017, 69-84.
[35] R. Chand, D. Yadav, G.C. Rana, Thermal instability of couple-stress nanofluid with vertical rotation in a porous medium, *Journal of Porous Media*, 20, 2017, 635-648.
[36] M. Sheikholeslami, D.D. Ganji, Heated permeable stretching surface in a porous medium using Nanofluids, *Journal of Applied Fluid Mechanics*, 7, 2014, 535-542.
[37] F. Selimefendigil, H.F. Öztop, Effects of nanoparticle shape on slot-jet impingement cooling of a corrugated surface with nanofluids, *Journal of Thermal Science and Engineering Applications*, 9, 2017, 021016.
[38] F. Selimefendigil, H.F. Öztop, Forced convection in a branching channel with partly elastic walls and inner L-shaped conductive obstacle under the influence of magnetic field, *International Journal of Heat and Mass Transfer*, 144, 2019, 118598.
[39] F. Selimefendigil, H.F. Öztop, MHD Pulsating forced convection of nanofluid over parallel plates with blocks in a channel, *International Journal of Mechanical Sciences*, 157-158, 2019, 726-740.
[40] J.C. Umavathi, D. Yadav, M.B. Mohite, Linear and nonlinear stability analyses of double-diffusive convection in a porous medium layer saturated in a Maxwell nanofluid with variable viscosity and conductivity, *Elixir Mech. Eng.,* 79, 2015, 30407-30426.
[41] I.S. Shivakumara, M. Dhananjaya, C.-O. Ng, Thermal convective instability in an Oldroyd-B nanofluid saturated porous layer, *International Journal of Heat and Mass Transfer*, 84, 2015, 167-177.
[42] P. Olson, P.G. Silver, R.W. Carlson, The large-scale structure of convection in the Earth's mantle, *Nature,* 344, 1990, 209.
[43] M. Fedi, F. Cella, M.D Antonio, G. Florio, V. Paoletti, V. Morra, Gravity modeling finds a large magma body in the deep crust below the Gulf of Naples, Italy, *Scientific Reports,* 8, 2018, 8229.
[44] C. Hirt, S. Claessens, T. Fecher, M. Kuhn, R. Pail, M. Rexer, New ultrahigh-resolution picture of Earth's gravity field, *Geophysical Research Letters*, 40, 2013, 4279-4283.

[45] B.D. Tapley, S. Bettadpur, J.C. Ries, P.F. Thompson, M.M. Watkins, GRACE measurements of mass variability in the Earth system, *Science*, 305, 2004, 503-505.
[46] S.M. Alex, P.R. Patil, Effect of variable gravity field on soret driven thermosolutal convection in a porous medium, *International Communications in Heat and Mass Transfer*, 28, 2001, 509-518.
[47] S.M. Alex, P.R. Patil, Effect of a variable gravity field on convection in an anisotropic porous medium with internal heat source and inclined temperature gradient, *Journal of Heat Transfer*, 124, 2002, 144-150.
[48] S. Govender, Coriolis effect on convection in a rotating porous layer subjected to variable gravity, *Transport in Porous Media*, 98, 2013, 443-450.
[49] U.S. Mahabaleshwar, D. Basavaraja, S. Wang, G. Lorenzini, E. Lorenzini, Convection in a porous medium with variable internal heat source and variable gravity, *International Journal of Heat and Mass Transfer*, 111, 2017, 651-656.
[50] D. Yadav, Numerical Investigation of the Combined Impact of Variable Gravity Field and Throughflow on the Onset of Convective Motion in a Porous Medium layer, *International Communications in Heat and Mass Transfer*,108, 2019, 104274.
[51] X. Liu, J. Pu, L. Wang, Q. Xue, Novel DLC/ionic liquid/graphene nanocomposite coatings towards high-vacuum related space applications, *Journal of Materials Chemistry A*, 1, 2013, 3797-3809.
[52] K.V. Wong, O. De Leon, Applications of nanofluids: current and future, in Nanotechnology and Energy, *Jenny Stanford Publishing*, 2017, pp. 105-132.
[53] D. Sui, V.H. Langåker, Z. Yu, Investigation of thermophysical properties of Nanofluids for application in geothermal energy, *Energy Procedia*, 105, 2017, 5055-5060.
[54] Q. Li, J. Wang, J. Wang, J. Baleta, C. Min, B. Sundén, Effects of gravity and variable thermal properties on nanofluid convective heat transfer using connected and unconnected walls, *Energy Conversion and Management*, 171, 2018, 1440-1448.
[55] R. Chand, G.C. Rana, S. Kumar, Variable gravity effects on thermal instability of nanofluid in anisotropic porous medium, *International Journal of Applied Mechanics and Engineering*, 18, 2013, 631-642.
[56] A. Mahajan, M.K. Sharma, Convection in a magnetic nanofluid saturating a porous medium under the influence of a variable gravity field, *Engineering Science and Technology, an International Journal*, 21, 2018, 439-450.
[57] D.A. Nield, A.V. Kuznetsov, Thermal instability in a porous medium layer saturated by a nanofluid: a revised model, *International Journal of Heat and Mass Transfer*, 68, 2014, 211-214.
[58] D. Yadav, D. Nam, J. Lee, The onset of transient Soret-driven MHD convection confined within a Hele-Shaw cell with nanoparticles suspension, *Journal of the Taiwan Institute of Chemical Engineers*, 58, 2016, 235-244.
[59] J. Buongiorno, Convective transport in nanofluids, *Journal of Heat Transfer*, 128, 2006, 240-250.
[60] D.A. Nield, A.V. Kuznetsov, The onset of convection in a horizontal nanofluid layer of finite depth, *European Journal of Mechanics - B/Fluids*, 29, 2010, 217-223.
[61] D. Yadav, Hydrodynamic and hydromagnetic instability in nanofluids, *Lap Lambert Academic Publishing*, 2014.
[62] P.G. Siddheshwar, C. Kanchana, Unicellular unsteady Rayleigh–Bénard convection in Newtonian liquids and Newtonian nanoliquids occupying enclosures: new findings, *International Journal of Mechanical Sciences*, 131, 2017, 1061-1072.
[63] M. Bouhalleb, H. Abbassi, Natural convection of nanofluids in enclosures with low aspect ratios, *International Journal of Hydrogen Energy*, 39, 2014, 15275-15286.
[64] S. Rionero, B. Straughan, Convection in a porous medium with internal heat source and variable gravity effects, *International Journal of Engineering Science*, 28, 1990, 497-503.
[65] M.S. Malashetty, M. Swamy, The effect of rotation on the onset of convection in a horizontal anisotropic porous layer, *International Journal of Thermal Sciences*, 46, 2007, 1023-1032.

ORCID iD

Dhananjay Yadav https://orcid.org/0000-0001-8404-2053

How to cite this article: Yadav D. The Density-Driven Nanofluid Convection in an Anisotropic Porous Medium Layer with Rotation and Variable Gravity Field: A Numerical Investigation, *J. Appl. Comput. Mech.*, 6(3), 2020, 699–712. https://doi.org/10.22055/JACM.2019.31137.1833